Clinicopathological Case Series of Four Patients with Inherited Macular Disease

Louisa Wickham,[1] Fred K. Chen,[1,2] Geoffrey P. Lewis,[3] Germit S. Uppal,[1] Magella M. Neveu,[4] Genevieve A. Wright,[1] Anthony G. Robson,[4] Andrew R. Webster,[2] Iain Grierson,[5] Paul Hiscott,[5] Peter J. Coffey,[2] Graham E. Holder,[4] Steven K. Fisher,[3] and Lyndon Da Cruz[1]

Purpose. To correlate the phenotype of four patients with inherited macular disease with the immunohistopathology of retinal tissue collected at the time of retinal pigment epithelium (RPE)–choroidal transplantation.

Methods. A clinicopathologic case series describing the phenotype of four patients, including confocal immunohistochemistry and electron microscopy (EM), and the results of genetic testing.

Results. In Case 1, electrophysiology showed only macular dysfunction. Confocal microscopy revealed minor abnormalities. EM showed abnormal cone inner segments with swollen mitochondria. In case 2 (R172W mutation in *RDS*), electrophysiology demonstrated generalized cone system dysfunction with severe macular involvement. Peripherin labeling of outer segments was nonuniform, and EM showed discs arranged in whorllike structures. Case 3 showed severe central macular dysfunction on multifocal electroretinogram (ERG). Peripherin staining was irregular and disorganized. EM revealed abnormal inner segment morphology, particularly in rods, and disorganized irregular outer segments. Case 4 had localized central macular dysfunction on multifocal ERG. Confocal microscopy was grossly normal, with evidence of early redistribution of cone opsin to the inner segment. EM showed variable rod morphology and normal cones.

Conclusions. RPE transplantation provides a unique opportunity to gain insight into retinal disorders by enabling phenotypic correlation with the immunohistopathology of retinal tissue collected during surgery. (*Invest Ophthalmol Vis Sci.* 2009;50:3553–3561) DOI:10.1167/iovs.08-2715

The inherited macular dystrophies are characterized by bilateral central visual loss and atrophy of the macula and underlying retinal pigment epithelium (RPE). They exhibit considerable clinical and genetic heterogeneity and are incompletely characterized.[1] Generalized photoreceptor dystrophies may also have macular involvement. To date, histopathologic study of human macular disease has been confined to post mortem specimens due to the difficulty in obtaining retinal samples.[2,3]

Macular translocation is a recognized therapeutic option for age-related macular degeneration and has been described in the treatment of adult-onset foveomacular vitelliform dystrophy.[4] RPE-choroidal transplantation has also shown potential as a surgical treatment for macular disease by transplanting healthier RPE and choroid from a more peripheral donor site to the macula. During this procedure, a small portion of peripheral neural retina is separated from the donor RPE–choroid patch and then removed from the eye, creating an opportunity for analysis of rapidly fixed retina in these patients.

A clinicopathologic case series is presented of four patients with inherited disease involving the macula who underwent RPE transplantation. A correlation between the phenotype and the immunohistopathology of retinal tissue collected during surgery has been performed in an attempt to aid in our understanding of these disorders.

Materials and Methods

This study received approval from the local Ethics Committee (ref. 05/Q0504/29) and adhered to the tenets of the Declaration of Helsinki.

Case Reports

Patients were ascertained from the medical retina clinics at Moorfields Eye Hospital. Four were considered suitable for RPE–choroid graft, and informed consent was obtained after a full explanation of the nature and possible consequences of the study.

Case 1. A 52-year-old man, reported a 4-year history of bilateral central visual loss. He had high myopia (−8-D spherical equivalent) with no relevant family history. One year before transplantation, left-eye visual acuity (VAL) declined over a 6-month period from 6/9 to 6/36 (logMAR 0.78). Over the following 6 months, right-eye visual acuity (VAR) deteriorated from 6/9 to 6/36 (logMAR 0.76) with loss of the ability to read. He denied photoaversion or nyctalopia.

Fundoscopy revealed irregular but sharply defined areas of atrophy of the RPE and inner choroid extending superiorly and inferiorly from the perifoveal region to the arcades with foveal pigmentary hyperplasia (Fig. 1A–D). The nasal retina had small yellow flecks at the level of the RPE but no pigmentary change or vascular sheathing. Both optic nerve heads were of normal appearance surrounded by a well-defined rim of peripapillary atrophy. Fixation was foveal and stable on the left but eccentric and unstable on the right.

Case 2. A 45-year-old man had presented at age 36 years with increased photosensitivity. His mother and maternal uncle were affected by rod–cone dystrophy. Electrophysiology at initial presentation was reported as normal. VAR declined over 2 years from 6/18 to 6/60 (logMAR 1.0), with eccentric fixation. Subsequently, over a 3-month period, VAL deteriorated from 6/12 to 6/18 (logMAR 0.44).

From the Departments of [1]Vitreoretinal Surgery and [4]Electrophysiology, Moorfields Eye Hospital, London, United Kingdom; the [2]Department of Cellular Therapy, UCL Institute of Ophthalmology, London, United Kingdom; the [3]Neuroscience Research Institute, University of California, Santa Barbara, California; and the [5]Unit of Ophthalmology, Department of Medicine, University of Liverpool, Liverpool, United Kingdom.

Supported by the Special Trustees of Moorfields Eye Hospital, the British Retinitis Pigmentosa Society, and the Foundation Fighting Blindness.

Submitted for publication August 13, 2008; revised December 1 and 30, 2008; accepted May 29, 2009.

Disclosure: **L. Wickham**, None; **F.K. Chen**, None; **G.P. Lewis**, None; **G.S. Uppal**, None; **M.M. Neveu**, None; **G.A. Wright**, None; **A.G. Robson**, None; **A.R. Webster**, None; **I. Grierson**, None; **P. Hiscott**, None; **P.J. Coffey**, None; **G.E. Holder**, None; **S.K. Fisher**, None; **L. Da Cruz**

The publication costs of this article were defrayed in part by page charge payment. This article must therefore be marked "*advertisement*" in accordance with 18 U.S.C. §1734 solely to indicate this fact.

Corresponding author: Louisa Wickham, Moorfields Eye Hospital, City Road, London, EC1V 2PD, UK; louisa.wickham@moorfields.nhs.uk.

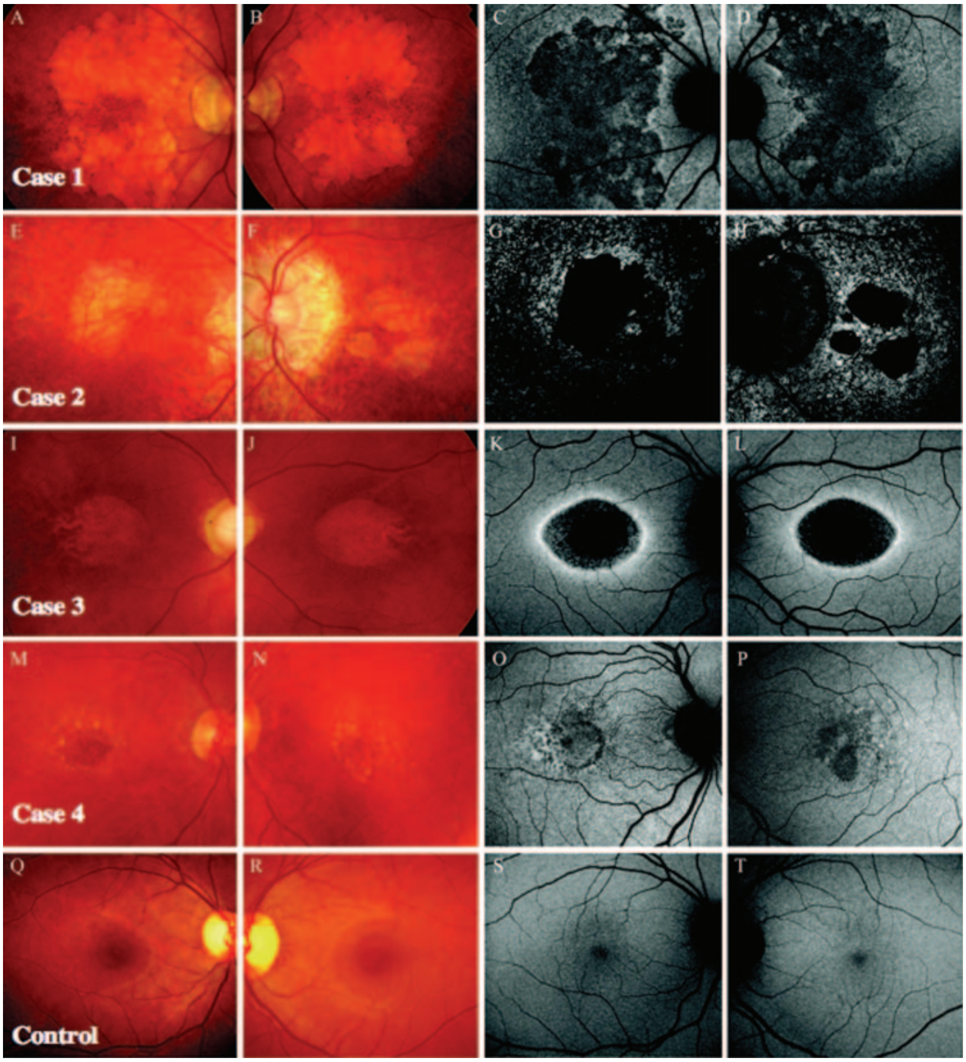

FIGURE 1. Color photographs and fundus autofluorescence images showing a variety of abnormalities. In autofluorescence images, hypo-autofluorescence (*black*) represents areas of RPE dysfunction and hyper-autofluorescence (*white*) is thought to indicate areas of distressed RPE cells. (**A–D**) Case 1: irregular but sharply defined areas of atrophy of the RPE and inner choroid extending superiorly and inferiorly from the perifoveal region to the arcades with foveal pigmentary hyperplasia (**A**, **B**). Abnormal central area of hypo-autofluorescence. (**E–H**) Case 2: well-defined areas of RPE and inner choroid atrophy at both maculae. (**I–L**) Case 3: bilateral bull's eye maculopathy with a small central island of RPE remaining on the right (**I**). (**M–P**) Case 4: yellow deposits at the level of the RPE in both maculae associated with pigmentary hyperplasia. A normal color fundus photograph and autofluorescence are shown for comparison (**Q–T**).

Ocular examination revealed well-defined areas of RPE and inner choroid atrophy at both maculae (Figs. 1E–H). In the left eye, three bands of intact RPE interrupted the area of atrophy meeting at the fovea. Prominent peripapillary atrophy was present. Peripheral retina, retinal vessels, and optic nerve heads were unremarkable.

Case 3. A 45-year-old man had presented at the age of 41 with progressive visual loss since his late 30s. He denied photoaversion or nyctalopia. He had no significant medical or ocular history. Direct questioning revealed a paternal great aunt who was blind by the age of 12. After presentation, his VAL improved from 2/60 to 6/36 over a period of 3 to 4 years as he adopted eccentric fixation. However, during the subsequent 12 months, VAR declined gradually from 6/9 to 6/36 (logMAR 0.82) with inability to read.

Examination of his anterior segments, lens, and vitreous were normal. Fundoscopy revealed bilateral bull's eye maculopathy with a small central island of RPE remaining on the right (Figs. 1I–L). The peripheral retina appeared healthy with no pigmentary or vascular abnormalities. Optic nerve heads were symmetrically cupped at 0.7 with no focal neuroretinal rim or nerve fiber layer loss.

Case 4. A 66-year-old woman presented with a 2-year history of bilateral sequential central visual loss. She denied photoaversion or nyctalopia. There was no relevant family history. At initial presentation, her fundus had a pseudovitelliform appearance. Over the next 18 months, VAR declined from 6/12 to 6/60. Over the following 6 months, VAL deteriorated from 6/12 to 6/24 (logMAR 0.60) with inability to read.

Ocular examination revealed normal anterior segments, clear lens, and vitreous. There were yellow deposits at the level of the RPE in both maculae associated with pigmentary hyperplasia (Figs. 1M–P). Peripheral retina, retinal vessels, and optic discs were normal.

A summary of the clinical features, genetic diagnosis and electrophysiology is given in Table 1.

Genetic Analysis

Blood samples were taken from the four patients and sent for genetic analysis at the Regional Molecular Genetics Laboratory, Manchester. Screening for Sorsby fundus dystrophy (SFD) was performed by bidirectional sequencing of the exon 5 and intron 4/exon 5 splice-acceptor site of the tissue inhibitor of metalloproteinases-3 (*TIMP-3*) gene. *RDS*/peripherin abnormalities were sought by bidirectional sequencing of the entire coding sequence of rhodopsin, including the intron/exon boundaries. Further samples were also sent to Asper Biotech (Tartu, Estonia) to look for variations in *ABCA4* using an arrayed primer extension genotyping array chip.

Preoperative Assessment

The patients underwent a full ophthalmic examination. Color fundus photography was captured as 8-bit digital images, and fundus autofluorescence images were obtained with a scanning laser ophthalmoscope (HRA 2; Heidelberg Engineering GmbH, Dossenheim, Germany) by using five to nine averaged images over a 30° field, which were then

Table 1. Summary of Findings for Each Case

	Case 1	Case 2	Case 3	Case 4
Age	48	36	Late 30's	64
Age at biopsy	52	45	45	66
Sex	M	M	M	F
Family History	Sporadic	Dominant	Sporadic	Sporadic
VA operated eye	0.76	0.44	0.82	0.60
Gene Identified		R172W		
Electrophysiology				
Cone ERG response	Normal	Subnormal	Normal	Normal
Rod ERG response	Normal	Normal	Mildly subnormal	Normal
Pattern ERG response	Absent	Absent	Absent	Normal
Rod Opsin	Localized to rod OS. Reduction in OS length and density.	Localized to rod OS. Reduction in OS length and density.	Localized to rod OS.	Localized to rod OS. Variable OS length and density.
M-cone opsin	Localized to cone OS. Reduction in OS length and density.	Localized to cone OS. Reduction in OS length and density.	Localized to cone OS. Variations in OS length.	Some areas of early redistribution to cone IS. Reduction in OS length and density.
Peripherin	Uniform staining of disc rims in OS.	Nonuniform staining. Clumps of peripherin within OS.	Staining irregular and disorganized	Uniform staining of disc rims in OS.
Cytochrome oxidase	Good staining of rod and cone IS	Normal	Normal	Normal
Calbindin-D	Good staining of horizontal cells, amacrine cells and labeling of cones.	Good staining of horizontal cells, amacrine cells and labeling of cones.	Marked decreased labeling of cones. Normal horizontal and amacrine cells.	Good staining of horizontal cells, amacrine cells and labeling of cones.
PNA	Normal interphotoreceptor matrix.	Normal	Normal	Normal
Synaptophysin	Normal cone synapse morphology.	Normal	Normal	Normal
7-G6	Normal cone labeling.	Normal	Normal	Normal
PKC	Normal rod bipolar cell morphology.	Normal	Normal	Normal
GFAP	Appeared increased; staining present within Müller cells from GCL to ONL.	Increased	Increased	Increased
EM	Abnormalities in cones greater than rods. Organized disc stacking but some abnormalities in OS structure.	Abnormal rods and cones. OS dysplastic with whorl-like structure.	Abnormalities in rods greater than cones. Disorganized OS structure.	Variable rod abnormalities, normal cones. Well organized OS disc structure.

averaged by using the image-analysis software provided (Heidelberg Eye Explorer).

Electrophysiology was performed on all patients to incorporate and exceed international standards and recommendations.[5–8] Pattern ERGs were recorded to an alternating checkerboard and the P50 component was used as a measure of macular function. Multifocal ERG responses to a scaled array of 61 stimulus hexagons covering a visual field of 57° were recorded, allowing assessment of localized cone system function over foveal and discrete paracentral areas. Full-field ERGs were used to assess generalized rod and cone system function under conditions of dark and light adaptation, respectively. Scotopic responses included the dim flash rod ERG and bright-flash maximum ERG; the latter a flash strength 0.6 log units greater than the standard flash ($3.0\ cd \cdot s \cdot m^{-2}$) to better demonstrate the ERG a-wave. Photopic cone system function was assessed with the 30-Hz flicker ERG and transient photopic ERG. The macula contributes minimally to full-field ERGs.

Collection of Retinal Specimens

Peripheral RPE-choroid transplantation was performed on all four patients by one surgeon (LdC) using a technique previously described.[9] In brief, a three-port pars plana vitrectomy was performed, a suitable site for RPE donation in the superior equatorial retina was identified, and diathermy was applied to a 2- to 3-mm^2 area. The neurosensory retina was then gently peeled off the surface of the RPE in two segments, removed from the eye, and immediately fixed. One segment was fixed in 4% Karnovsky solution for electron microscopy and the other in 4% paraformaldehyde solution for confocal microscopy.

Immunohistochemistry

After a rinse in PBS, the specimens that had been fixed in paraformaldehyde were embedded in 5% agarose (Sigma-Aldrich, St. Louis, MO) in sodium phosphate buffer (PBS). Seventy-five-micrometer-thick sections were cut with a vibratome (Technical Products International, Polysciences, Warrington, PA) and incubated in normal donkey serum (1:20; Jackson ImmunoResearch, West Grove, PA) in PBTA (i.e., PBS containing 0.5% bovine serum albumin (BSA; Fisher Scientific, Pittsburgh, PA), 0.1% Triton X-100 (Boehringer Mannheim, Indianapolis, IN), and 0.1% sodium azide (Sigma-Aldrich) overnight at 4°C on a rotator. After removal of the blocking serum, primary antibodies were added (Table 2).

After overnight incubation at 4°C on a rotator, sections were rinsed in PBTA and incubated again overnight at 4°C with the secondary antibodies. Donkey anti-mouse and donkey anti-rabbit secondary antibodies were used for each combination of primary antibodies, conju-

Table 2. Antibodies

Antibody	Manufacturer	Concentration
α Calbindin-D	Sigma (St Louis, MO)	1:1000
α GFAP	Dako (Carpinteria, CA)	1:400
α Synaptophysin	Dako	1:100
αM-cone opsin	Chemicon International (Temecula, CA)	1:500
αPKC	Biomol Research Labs, Inc. (Plymouth Meeting, PA)	1:100
α Rhodopsin	Santa Cruz Biotechnology, Inc. (Santa Cruz, CA)	1:100
PNA-biotin	Vector Laboratories (Burlingame, CA)	1:1000
α Cytochrome oxidase	Molecular Probes (Eugene, OR)	1:100
α Peripherin 3B6	Robert Molday, University of British Columbia (Vancouver, BC, Canada)	1:10
α 7G6	Peter MacLeish, Morehouse School of Medicine (Atlanta, GA); Wolfgang Baehr, University of Utah (Salt Lake City, UT)	1:100

gated to Cy2 or Cy3 (Jackson ImmunoResearch). All secondary antibodies were used at a dilution of 1:200, and all the antibodies were diluted in PBTA. The sections were then rinsed, mounted in *N*-propyl gallate in glycerol and viewed on a laser scanning confocal microscope (Fluoview 500; Olympus, Tokyo, Japan).

Transmission Electron Microscopy

The specimens that had been fixed in Karnovsky solution were rinsed in buffer, dehydrated in a graded ethanol series, placed in 100% resin for 6 hours with rotation, and embedded and cured overnight in a 60°C oven.

Semithin (1 μm) sections for light microscopy and ultrathin (70 nm) sections for transmission electron microscopy (TEM) were cut with a microtome (Ultracut S; Leica, Deerfield, IL) fitted with a diamond knife. Semithin sections were stained with alcoholic toluidine blue. Ultrathin sections were contrasted by sequential staining with saturated uranyl acetate in 50% ethanol followed by lead citrate and viewed and photographed in a transmission electron microscope operating at 80 kV (model 1010; JEOL; Peabody, MA).

Results

Genetic Analysis

In cases 1, 3, and 4, genetic analysis revealed no mutation in any of the genes tested. Genetic analysis of case 2 revealed an R172W mutation in the *RDS* gene.

Electrophysiology

Case 1. Full-field and pattern ERGs were performed at 1 month (Fig. 2), 1 year, and 2 years before transplantation. Multifocal ERG was performed at 1 month before transplantation. Visual acuity was 6/9 in each eye at the time of the initial two recordings and 6/36 VAR and 3/36 VAL at the latest recording. Undetectable pattern ERGs (Fig. 2) and central multifocal ERG (Fig. 3) abnormalities, consistent with central macular dysfunction, were observed in both eyes. Full-field ERGs showed no electrophysiological evidence of generalized retinal involvement.

Case 2. Full-field, pattern, and multifocal ERGs were performed on two occasions: 2 weeks (Fig. 2) and 2 years before transplantation. VAR was 6/18 and VAL was 6/12 on that occasion. The full-field ERGs were consistent with a loss of generalized cone system function but rod-mediated ERGs were normal. This result was confirmed in a second ERG. Pattern and multifocal ERGs were consistent with severe macular involvement (Figs. 2, 3).

Case 3. Full-field and pattern ERGs were performed at 2 weeks (Fig. 2) and 4 years before transplantation. Multifocal ERGs were performed 2 weeks before transplantation (Fig. 3). VAR was 6/9 and VAL was CF at the time of the initial recording but had deteriorated to 6/60 and 6/36, respectively, before surgery. At presentation, residual pattern ERGs were present, but immediately before RPE transplantation, these were undetectable and there was severe multifocal ERG reduction consistent with severe central macular dysfunction (Fig. 3). Full-field ERGs had some mildly abnormal features suggestive of dysfunction occurring after phototransduction, although the a-wave in the bright-flash ERG was normal. There was no evidence of generalized rod photoreceptor or cone system dysfunction.

Case 4. Full-field, pattern, and multifocal ERGs were performed at 1 day (Figs. 2, 3) and 3 months before transplantation. VA was 6/60 in each eye on both occasions. Pattern ERGs immediately before surgery were normal in the surgical eye but multifocal ERGs confirmed the presence of localized central macular dysfunction (Fig. 3). There was no multifocal ERG evidence of peripheral macular cone system involvement and full-field ERGs were within age-matched normal limits bilaterally.

Confocal Microscopy

Case 1. Confocal microscopy, showed normal distribution of protein in cones (M-cone opsin) and rods (rod opsin), although there were areas where the outer segments (OS) appeared reduced in length and density (Fig. 4A, M cone opsin red; Fig. 5A, rod opsin red; Table 2). Normal cytochrome oxidase labeling in both rod and the larger cone inner segments (IS; Fig. 4A, green) was observed. Labeling of rod OS with peripherin suggested normal morphology with uniform staining of the disc rims in the OS (Fig. 5A; peripherin, green; rod opsin, red). Normal cone morphology and interphotoreceptor matrix was shown by labeling with anti-calbindin D and biotinylated peanut agglutinin (PNA) respectively (Fig. 4B calbindin D, green; Fig. 4D PNA, red). Normal cone synapse morphology was demonstrated with synaptophysin, which labels synaptic vesicle proteins in synaptic terminals (Fig. 4C, green), and anti-7G6, which labels cone arrestin in the entire cone (Fig. 4C, red). Labeling with anti-7G6 also showed rounded-off cone OS (Fig. 4C, arrow). Anti-calbindin D labels horizontal and amacrine cells in the INL, and the labeling was grossly normal (Fig. 4B, green). Similarly the morphology of the rod bipolar cells, demonstrated with anti-protein kinase C (PKC), was unremarkable (Fig. 4B, red). Glial fibrillary acidic protein (GFAP) expression was present throughout the ganglion cell layer to the outer nuclear layer within Müller cells (Fig. 4D, green) and appeared increased compared with that in normal retinas.[10,11]

Case 2. Both anti-M-cone– and rod opsin–labeled OS appeared reduced in length (Fig. 4E, cone opsin, red; Fig. 4H, rod opsin, red). In some areas, there was evidence of early redistribution of cone opsin to the IS (Fig. 4E, arrow). Peripherin labeling of rod OS disc rims was nonuniform, with clumps of

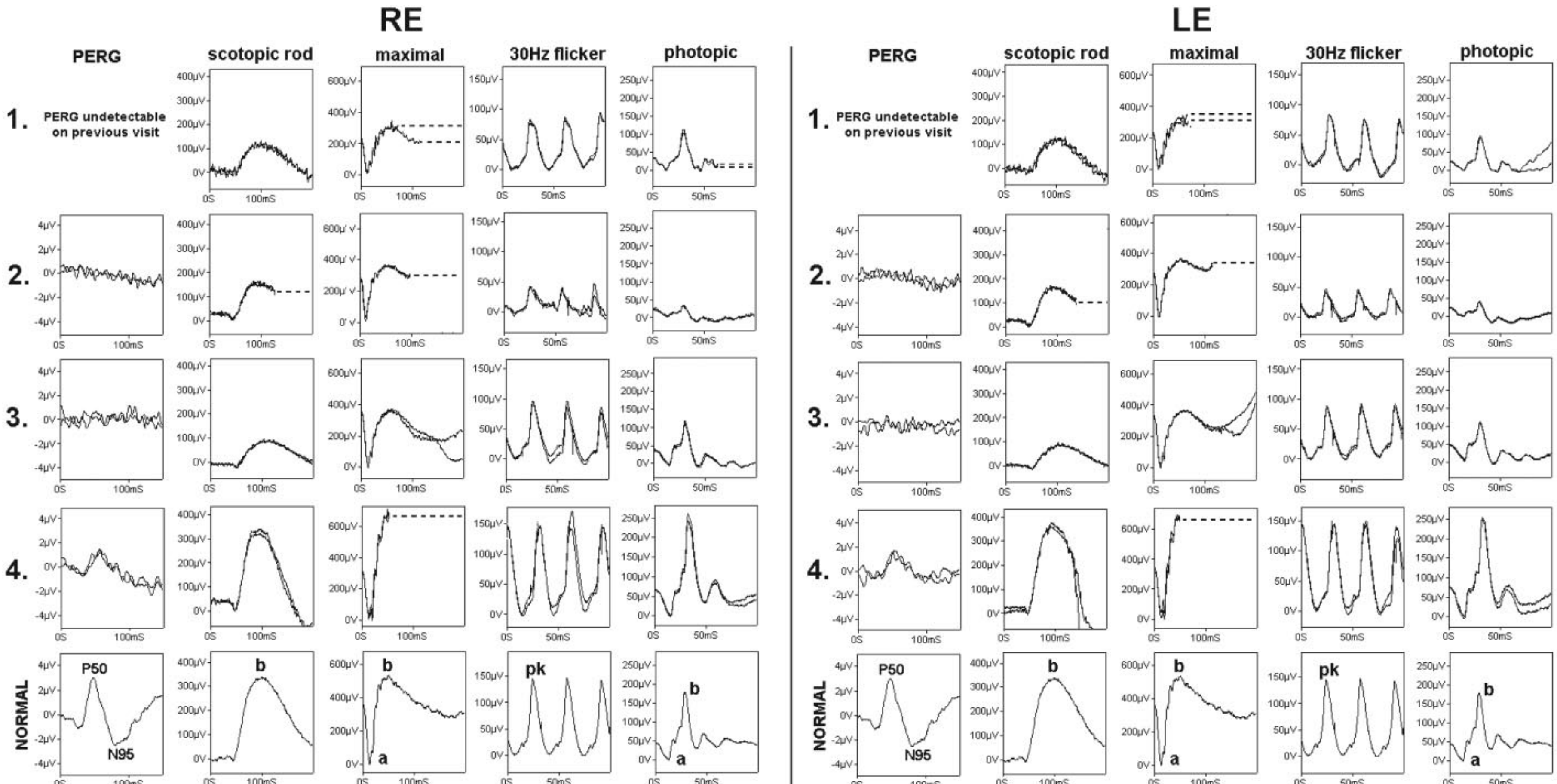

Figure 2. Pattern and full-field ERGs recorded before surgery in cases 1 to 4. A normal example is shown for comparison (*bottom row*). Case 1: full-field ERGs were normal in both eyes. Case 2: pattern ERG was undetectable in both eyes; scotopic ERGs were normal but cone-mediated photopic ERGs were of subnormal amplitude in both eyes. Case 3: pattern ERG was undetectable in both eyes. The scotopic ERG was mildly subnormal in both eyes. The maximum ERG a-wave was normal, but the b wave was mildly subnormal bilaterally. Cone-mediated ERGs were normal in both eyes. Case 4: pattern ERG and all full-field ERGs were normal in both eyes.

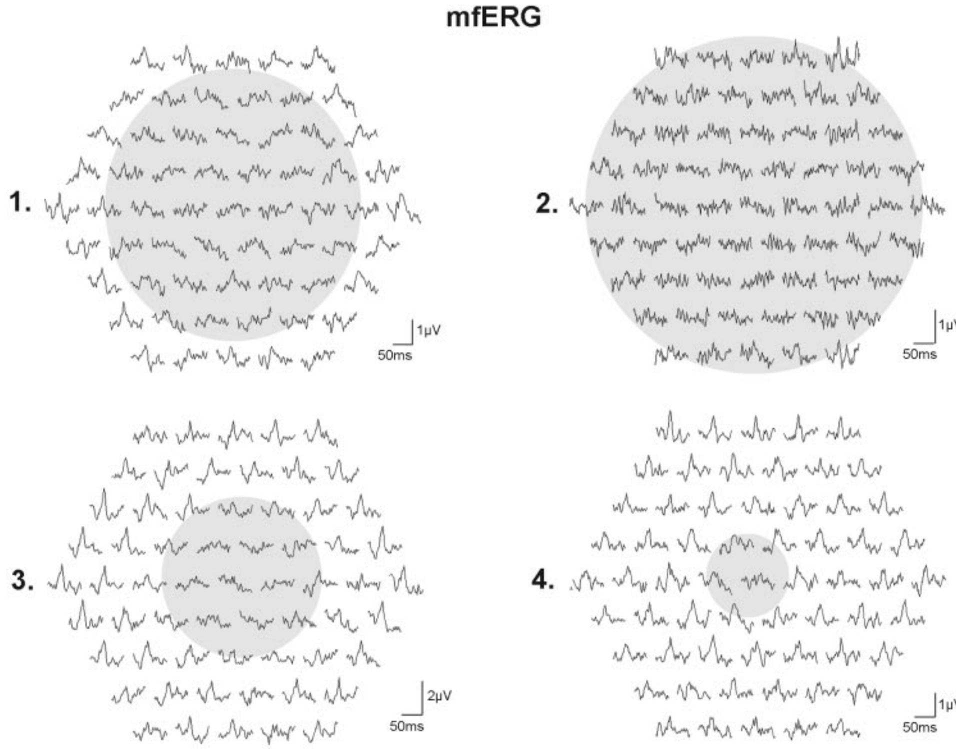

Figure 3. Multifocal ERG traces in the surgical eye. Multifocal ERGs are shown with a high scaling factor to optimally illustrate small responses. Case 1: markedly abnormal responses to the central hexagons with some preservation over the most eccentric areas. Case 2: widespread abnormal responses. Case 3: markedly abnormal responses to central and paracentral hexagons, with preservation of more eccentric responses. Case 4: abnormal responses localized to central and discrete paracentral areas. *Shaded area*: approximate areas of significant mfERG reduction.

peripherin observed within the OS (Fig. 5D, green, arrows). There was generalized increased distribution in labeling of Müller cells with GFAP (Fig. 4H, green). Findings are summarized in Table 2.

Case 3. The staining of rod OS with peripherin was irregular and disorganized (Fig. 5G, green; Table 2). Labeling of cones with anti-calbindin D was markedly reduced or absent; however, staining of horizontal and amacrine cells appeared normal (Fig. 4J; anti-calbindin D, green). Distribution of anti-GFAP labeling in Müller cells was generally increased (Fig. 4L, green).

Case 4. Cone OS structure was variable, with some being of normal length and others being shortened (Fig. 4M, red). In some areas there was evidence of early redistribution of cone opsin to the IS (Fig. 4M, arrow). Labeling with peripherin and rod opsin was grossly normal (Fig. 4J, peripherin green, rod opsin red). Staining with GFAP was increased and occasionally Müller cell end feet were seen to breach the outer limiting membrane (OLM; Fig. 4P, arrow).

Electron Microscopy

Case 1. TEM revealed abnormal cone IS with swollen mitochondria and apoptotic cell bodies (Fig. 5C, arrow). These abnormalities appeared to affect cones preferentially, with adjacent rod IS being relatively spared. Most OS were detached from their IS, although this may be an artifact of the detachment and sectioning procedures. Many appeared to be relatively normal with well-organized discs, but in others the discs were stacked in an inconsistent fashion (Fig. 5B).

Case 2. There were generalized abnormalities of both rod and cone structure, although rods appeared to be more severely affected, with mitochondria being grossly swollen (Fig. 5F). OS were dysplastic with distortion of discs into whorl structures (Fig. 5E, arrow).

Case 3. The cone IS morphology appeared to be abnormal; however, abnormalities in morphology were more marked in the rod population (Fig. 5I). In the rod IS the mitochondria were swollen and reduced in number. The OS were of variable size and shape with disorganized disc structure (Fig. 5H).

Case 4. Cone morphology was normal (Fig. 5L), but rod morphology was variable, with some appearing grossly normal and others appearing atrophic or with abnormal, swollen mitochondria (arrow). The OS were also grossly normal with well-organized disc structure (Fig. 5K).

A summary of the findings are presented in Table 2.

Discussion

To our knowledge, this represents the first opportunity to study relatively well-preserved retinas of patients with inherited retinal disease involving the macula. The tissue was not from postmortem eyes but was obtained during surgery and placed immediately in fixative. Immunohistochemical and structural abnormalities in the peripheral retina of these four patients are discussed in relation to the electrophysiological findings.

In case 1, electrophysiology indicated a disease primarily of macular cone function, with no evidence of generalized retinal involvement. Marked abnormalities of cone IS mitochondria with relative sparing of the rods was observed on TEM. Confocal microscopy, however, showed little alteration in retinal structure apart from a slight reduction in OS length and an increased distribution of GFAP expression. Despite the presence of grossly abnormal cone mitochondria, labeling with cytochrome oxidase appeared to be normal by confocal microscopy. It is therefore possible that the findings demonstrated by TEM indicate subclinical disease with vulnerable, diseased cells, in this case cones, being more susceptible to oxidative stress during fixation. Although mild GFAP staining can be found in normal retinas, strong GFAP labeling was observed in all four of the retinal samples in this study, this is a nonspecific indicator of stress and may occur in response to several retinal diseases, including age-related macular degeneration.[10,12–15] In one report, cone pedicles were also enlarged, but this was not found in our study (data not shown).[16]

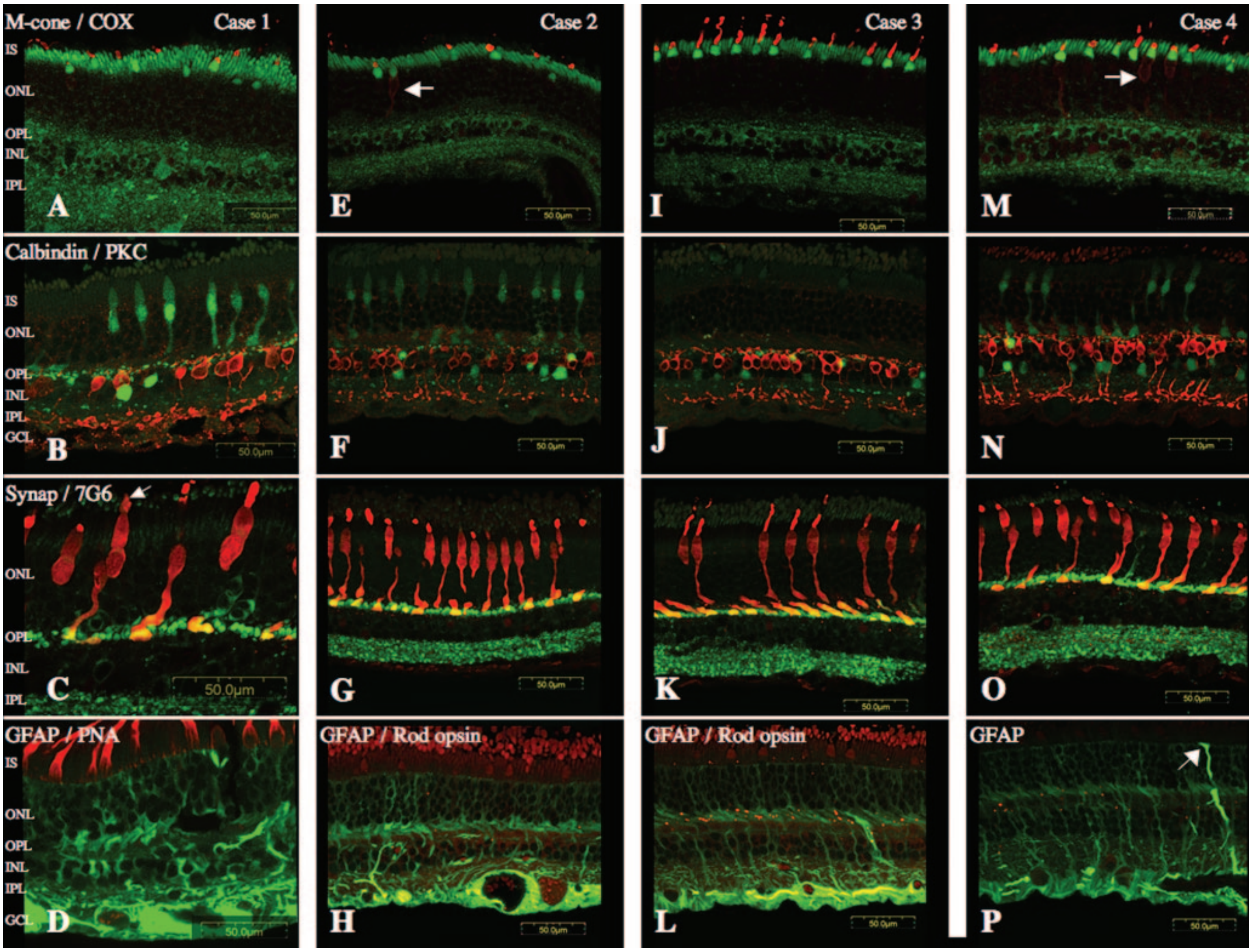

Figure 4. Double-labeled laser scanning confocal images showing changes in the distribution of several proteins in four patients with inherited macular disease. (**A**, **E**, **I**, **M**, *red*) Normal distribution of M-cone opsin in three patients, labeling the OS only. Patients 2 (**E**) and 4 (**M**) showed evidence of early redistribution to the IS (*arrow*). (**A**, **E**, **I**, **M**, *green*) Cytochrome oxidase (COX) showed normal labeling of mitochondria in rod and cone IS. (**B**, **F**, **J**, **N**, *green*) Calbindin D labels cones and horizontal and amacrine cells in the inner nuclear layer (INL). Labeling was markedly reduced or absent in patient 3 (**J**) but was normal in the other three patients. (**B**, **F**, **J**, **N**, *red*) PKC labeling of rod bipolar cells appeared normal in all four patients. (**C**, **G**, **K**, **O**, *green*) Synaptophysin M, which labels rod and cone synaptic terminals in the outer plexiform layer (OPL), and (**C**, **G**, **K**, **O**, *red*) 7G6, which labels cone arrestin in the entire cone, appeared normal in all patients. (**D**, **H**, **L**, **P**, *green*) GFAP was present throughout the ganglion cell layer (GCL) to the outer nuclear layer (ONL) within Müller cells and appeared to be increased in all patients. In patient 4, occasional Müller cell end feet breached the OLM (**P**, *arrow*). (**H**, **L** *red*) Rod opsin showed a normal distribution in all patients and was limited to the OS. There was a reduction in OS length and density in all patients. (**D**, *red*) Biotinylated PNA labels cone sheaths, a component of the extracellular matrix associated with cone photoreceptors. Labeling was normal in all patients (data not shown for patients 2–4).

Patient 2 was found to have an R172W mutation in the *RDS* gene, a condition in which the clinical and ERG phenotype is variable.[17] In this case, the electrophysiology was consistent with generalized loss of retinal function confined to the cone system with severe macular involvement. Similar ERG findings have been previously reported in association with the R172W mutation.[18] Peripherin/rds and rom1 are transmembrane proteins localized to rod OS disc rims and are involved in disc morphogenesis and maintenance of OS structure. In case 2, abnormalities of peripherin staining in rod photoreceptor OS were observed on confocal microscopy. Kedzierski et al.[19] described whorllike structures in rod OS of transgenic mice with RDS mutations, similar to those described in this study on TEM, and proposed that whorls result from the insufficiency of peripherin/rds which causes disc enlargement. Others have hypothesized that it may reflect disruption of other interactions required for maintenance of rod OS.[20] Rod neurite sprouting has also been reported in cases of *RDS* mutation,[21,22] but was not observed in this study.

In case 3 the rod specific ERG, arising in the ON-bipolar cells was subnormal. However, a normal a-wave in the bright flash ERG confirmed that the process of phototransduction was not compromised. Further examination of the ERGs showed a subnormal rod ERG and a maximum response with a low b- to a-wave ratio, suggestive of dysfunction occurring after phototransduction. Irregular peripherin staining of the rod OS was consistent with the disorganized disc structure observed on TEM. Reduced labeling with calbindin D, a calcium binding protein found in cones, but not rods, of many animal species, was observed in this case. The importance of this finding is difficult to determine, as calbindin expression in the human retina varies, being reduced or absent in the fovea or parafovea, but prevalent in the perifovea and peripheral retina.[23] Variations in anti-calbindin labeling similar to that seen in this

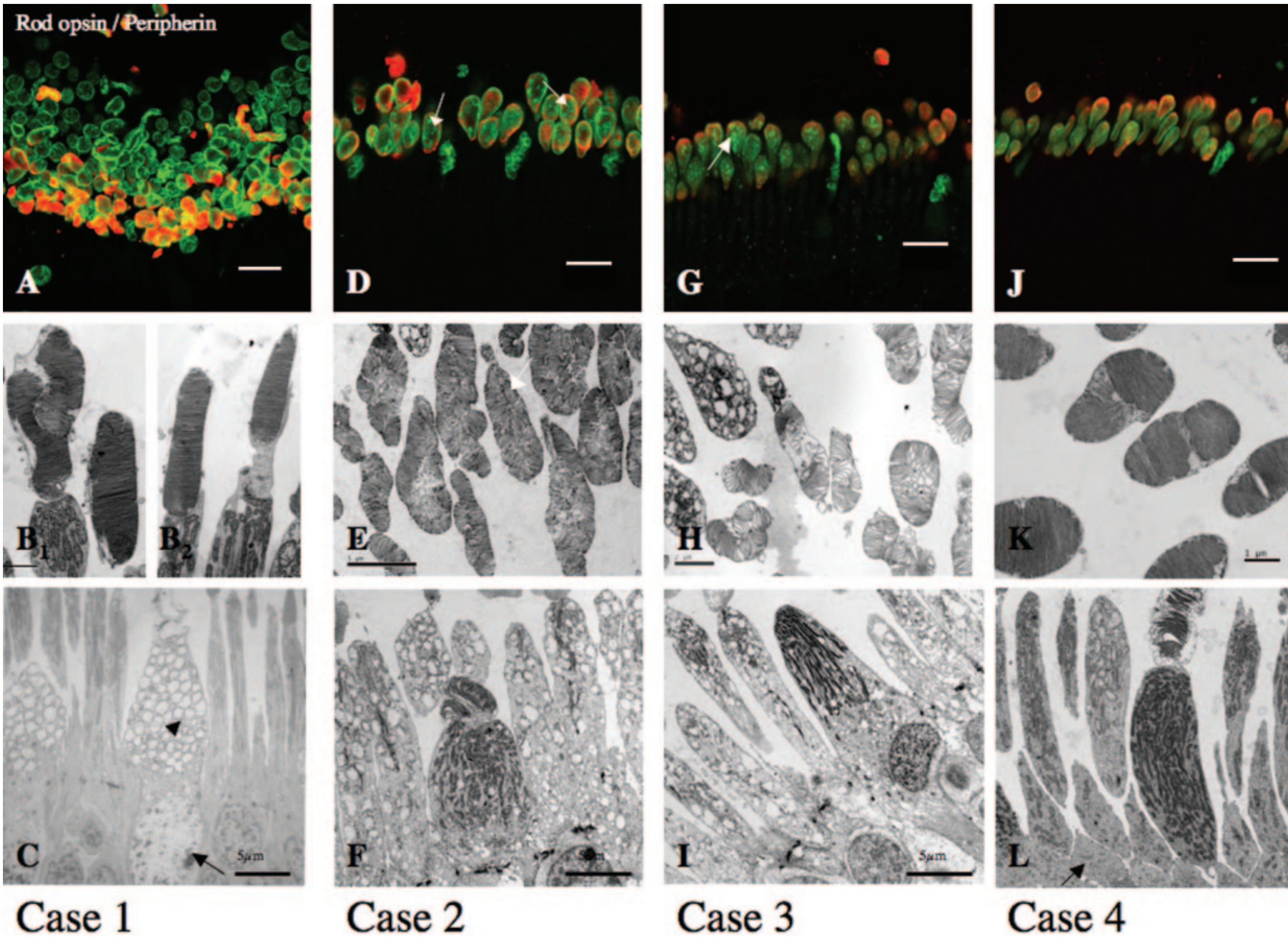

FIGURE 5. Double-label laser scanning confocal microscopy and TEM showing changes in photoreceptor morphology in four patients with inherited macular disease. (**A**, **D**, **G**, **J**) Confocal images of peripherin (*green*) labels rod OS disc rims. Scale bar, 10 μm. Patients 1 and 4 (**A**, **J**) showed uniform staining of disc rims suggesting normal morphology. Patients 2 and 3 (**D**, **G**) demonstrated nonuniform clumps of peripherin (*arrows*) within the OS. (**A**, **D**, **G**, **J**) Rod opsin staining (*red*) of rod OS appeared normal in all patients. (**B**, **E**, **H**, **K**) TEM of OS showed grossly normal morphology in patients 1 and 4 (**B**, **K**). (**B_1**) An area of disorganized disc stacking with abnormalities in structure. In some areas the OS appeared to be relatively normal with well organized discs (**B_2**). Scale bar, 1 μm. Patient 2 (**E**) demonstrates dysplastic OS with distortion of discs into whorllike structures (*arrow*). Scale bar, 5 μm. Patient 3 (**H**) shows OS of variable size and shape with disorganized disc structure. Scale bar, 2 μm. (**C**, **F**, **I**, **L**) TEM of rods and cones. Scale bar, 5 μm. Swollen mitochondria were present in all patients, but the distribution varied among patients. Patient 1 (**C**) showed swollen mitochondria in cone IS (*arrowhead*) with adjacent rods being relatively spared. Apoptotic cell bodies were also seen in this patient (*arrow*). Patients 2 and 3 (**F**, **I**) appeared to have more marked abnormalities in the rod population. In patient 4 (**L**), cone morphology was grossly normal, with variable involvement of the rod population.

study (i.e., reduced labeling of cones and normal labeling of horizontal and amacrine cells) have also been noted in patients with retinitis pigmentosa[22] and in those with retinal detachment.[24,25]

In case 4, electrophysiological abnormalities were confined to the central macula. TEM of the equatorial retinal sample was grossly normal, consistent with full-field ERGs that were within age-matched normal limits. On fundoscopy, this patient was noted to have multiple yellow deposits at the level of the RPE in both maculae. Shortening of photoreceptor OS and isolated areas of cone opsin redistribution were observed on confocal microscopy and similar changes have also been described in photoreceptors overlying drusen in patients with age-related macular degeneration as well as retinal detachment.[24,26]

Phenotypic variation of the *ABCA4* gene is profound and is involved in several retinal dystrophies including Stargardt fundus flavimaculatus, retinitis pigmentosa, cone rod dystrophy and AMD.[1,27] It is therefore conceivable that patients in this study may have had a mutation in *ABCA4*. Analysis of the ABCA4 gene was performed with a micorarray gene chip designed to screen for known mutations in the gene; no patient studied had mutations detected. Although this chip is regularly updated and at the time of analysis was able to test >98% of the known genetic variations, screening of the *ABCA4* gene is complicated by its large size and allelic heterogeneity with many polymorphisms, making it difficult to be certain that no disease-causing mutation exists.[28]

The patients in this study presented with macular disease, but the samples obtained at the time of surgery were from the equatorial retina. Gene expression at the fovea may differ from that in the peripheral retina,[29,30] possibly reflecting structural differences such as the high density of ganglion cells at the macula, and it therefore cannot be excluded that other abnormalities of photoreceptors and neural retina may exist in this region. Further, this study was confined to the analysis of the neural retina and offers no insight into the structure of the RPE or its interaction with photoreceptors. All the retinal samples were collected at the time of transplantation surgery, and although the neural retina was separated carefully from the underlying RPE, the sampling process may have caused cellular damage. It would be expected that such artifacts would occur uniformly in rods and cones and is therefore unlikely to explain the differences observed in this study.

In this study, multifocal ERGs detected localized areas of cone system dysfunction, and it is possible that wider field multifocal ERG would better evaluate the function of potential graft sites before surgery. The need to perform full-field ERG is clearly demonstrated, as patients with a fundus appearance thought to reflect a macular dystrophy may show electrophysiological evidence of generalized retinal dysfunction.

In conclusion, samples obtained during transplantation surgery in these four patients with predominantly macular disease have enabled a correlation to be determined between histology and function in living eyes. There was a range of retinal disease in the equatorial retina, reflecting the underlying diseases. Retinal transplantation provides a unique opportunity to assess retinal tissue, allowing further characterization of retinal disease and dysfunction.

Acknowledgments

The authors thank the Macular Disease Society of the United Kingdom for allowing us to perform the genotyping of *ABCA4* gene and the EVI-Genoret Consortium for the infrastructure used in reviewing the patients.

References

1. Michaelides M, Hunt DM, Moore AT. The genetics of inherited macular dystrophies. *J Med Genet.* 2003;40:641–650.
2. Rabb MF, Tso MO, Fishman GA. Cone-rod dystrophy: a clinical and histopathologic report. *Ophthalmology.* 1986;93:1443–1451.
3. Dubovy SR, Hairston RJ, Schatz H, et al. Adult-onset foveomacular pigment epithelial dystrophy: clinicopathologic correlation of three cases. *Retina.* 2000;20:638–649.
4. Eckardt C, Eckardt U, Groos S, Luciano L, Reale E. Macular translocation in a patient with adult-onset foveomacular vitelliform dystrophy with light- and electron-microscopic observations on the surgically removed subfoveal tissue. *Graefes Arch Clin Exp Ophthalmol.* 2004;242:456–467.
5. Bach M, Hawlina M, Holder GE, et al. Standard for pattern electroretinography. International Society for Clinical Electrophysiology of Vision. *Doc Ophthalmol.* 2000;101:11–18.
6. Holder GE, Brigell MG, Hawlina M, Meigen T, Vaegan, Bach M. ISCEV standard for clinical pattern electroretinography: 2007 update. *Doc Ophthalmol.* 2007;114:111–116.
7. Marmor MF, Hood DC, Keating D, Kondo M, Seeliger MW, Miyake Y. Guidelines for basic multifocal electroretinography. *Doc Ophthalmol.* 2003;106:105–115.
8. Marmor MF, Holder GE, Seeliger MW, Yamamoto S. Standard for clinical electroretinography (2004 update). *Doc Ophthalmol.* 2004;108:107–114.
9. van Meurs J, Van den Biesen PR. Autologous retinal pigment epithelium and choroid translocation in patients with exudative age-related macular degeneration: short-term follow-up. *Am J Ophthalmol.* 2003;136:688–695.
10. Wu KH, Madigan MC, Billson FA, Penfold PL. Differential expression of GFAP in early v late AMD: a quantitative analysis. *Br J Ophthalmol.* 2003;87:1159–1166.
11. Wu KH, Penfold PL, Billson FA. Effects of post-mortem delay and storage duration on the expression of GFAP in normal human adult retinae. *Clin Exp Ophthalmol.* 2002;30:200–207.
12. Reilly JF, Maher PA, Kumari VG. Regulation of astrocyte GFAP expression by TGF-beta1 and FGF-2. *Glia.* 1998;22:202–210.
13. Nork TM, Ghobrial MW, Peyman GA, Tso MO. Massive retinal gliosis: a reactive proliferation of Muller cells. *Arch Ophthalmol.* 1986;104:1383–1389.
14. Mizutani M, Gerhardinger C, Lorenzi M. Muller cell changes in human diabetic retinopathy. *Diabetes.* 1998;47:445–449.
15. Lewis GP, Erickson PA, Guerin CJ, Anderson DH, Fisher SK. Basic fibroblast growth factor: a potential regulator of proliferation and intermediate filament expression in the retina. *J Neurosci.* 1992;12:3968–3978.
16. Gregory-Evans K, Fariss RN, Possin D, Gregory-Evancs CY, Milam AH. Abnormal cone synapses in human cone-rod dystrophy. *Ophthalmology.* 1998;105:2306–2312.
17. Michaelides M, Holder GE, Bradshaw K, Hunt DM, Moore AT. Cone-rod dystrophy, intrafamilial variability, and incomplete penetrance associated with the R172W mutation in the peripherin/RDS gene. *Ophthalmology.* 2005;112:1592–1598.
18. Downes SM, Fitzke FW, Holder GE, et al. Clinical features of codon 172 RDS macular dystrophy: similar phenotype in 12 families. *Arch Ophthalmol.* 1999;117:1373–1383.
19. Kedzierski W, Lloyd M, Birch DG, Bok D, Travis GH. Generation and analysis of transgenic mice expressing P216L-substituted rds/peripherin in rod photoreceptors. *Invest Ophthalmol Vis Sci.* 1997;38:498–509.
20. Tam BM, Moritz OL, Papermaster DS. The C terminus of peripherin/rds participates in rod outer segment targeting and alignment of disk incisures. *Mol Biol Cell.* 2004;15:2027–2037.
21. Li ZY, Kljavin IJ, Milam AH. Rod photoreceptor neurite sprouting in retinitis pigmentosa. *J Neurosci.* 1995;15:5429–5438.
22. Fariss RN, Li ZY, Milam AH. Abnormalities in rod photoreceptors, amacrine cells, and horizontal cells in human retinas with retinitis pigmentosa. *Am J Ophthalmol.* 2000;129:215–223.
23. Haley TL, Pochet R, Baizer L, et al. Calbindin D-28K immunoreactivity of human cone cells varies with retinal position. *Vis Neurosci.* 1995;12:301–307.
24. Sethi CS, Lewis GP, Fisher SK. Glial remodelling and neuronal plasticity in human retinal detachment with proliferative vitreoretinopathy. *Invest Ophthalmol Vis Sci.* 2005;46:329–342.
25. Rex TS, Fariss RN, Lewis GP, Linberg KA, Sokal I, Fisher SK. A survey of molecular expression by photoreceptors after experimental retinal detachment. *Invest Ophthalmol Vis Sci.* 2002;43:1234–1247.
26. Johnson PT, Lewis GP, Talaga KC, et al. Drusen-associated degeneration in the retina. *Invest Ophthalmol Vis Sci.* 2003;44:4481–4488.
27. Valverde D, Riveiro-Alvarez R, Aguirre-Lamban J, et al. Spectrum of the *ABCA4* gene mutations implicated in severe retinopathies in Spanish patients. *Invest Ophthalmol Vis Sci.* 2007;48:985–990.
28. Valverde D, Riveiro-Alvarez R, Bernal S, et al. Microarray-based mutation analysis of the ABCA4 gene in Spanish patients with Stargardt disease: evidence of a prevalent mutated allele. *Mol Vis.* 2006;12:902–908.
29. Bernstein SL, Borst DE, Neuder ME, Wong P. Characterization of a human fovea cDNA library and regional differential gene expression in the human retina. *Genomics.* 1996;32:301–308.
30. Sharon D, Blackshaw S, Cepko CL, Dryja TP. Profile of the genes expressed in the human peripheral retina, macula, and retinal pigment epithelium determined through serial analysis of gene expression (SAGE). *Proc Natl Acad Sci U S A.* 2002;99:315–320.